Reprinted from
Journal of Imaging Science and Technology® 62(4): 040406-1–040406-6, 2018.

Piezoelectric Inkjet-Printed Metallic Igniters

Allison K. Murray, Whitney A. Novotny, and Nikhil Bajaj
School of Mechanical Engineering, Purdue University, West Lafayette, IN 47907, USA
Ray W. Herrick Laboratories, Purdue University, West Lafayette, IN 47907, USA

I. Emre Gunduz and Steven F. Son
School of Mechanical Engineering, Purdue University, West Lafayette, IN 47907, USA
Maurice J. Zucrow Laboratories, Purdue University, West Lafayette, IN 47907, USA

George T.-C. Chiu
School of Mechanical Engineering, Purdue University, West Lafayette, IN 47907, USA
Ray W. Herrick Laboratories, Purdue University, West Lafayette, IN 47907, USA

Jeffrey F. Rhoads
School of Mechanical Engineering, Purdue University, West Lafayette, IN 47907, USA
Ray W. Herrick Laboratories, Purdue University, West Lafayette, IN 47907, USA
Birck Nanotechnology Center, Purdue University, West Lafayette, IN 47907, USA
E-mail: jfrhoads@purdue.edu

Abstract. *This work demonstrated printed metallic bridge wire and spark gap igniters suitable for use with energetic materials. These devices were fabricated from an aqueous dispersion of silver nanoparticles on a flexible, mesoporous substrate using a piezoelectric inkjet printer. This manufacturing process resulted in precise samples fabricated without the need for thermal curing. Geometric parameters were varied for the devices to determine the design criteria of importance and to quantify the electrical excitation needed for optimal performance. The work successfully demonstrated the integration of bridge wires and spark gaps with energetic material to produce fully printed igniters that are of practical use in applications ranging from munitions to vehicle airbags.* © *2018 Society for Imaging Science and Technology.*
[DOI: 10.2352/J.ImagingSci.Technol.2018.62.4.040406]

1. INTRODUCTION

Initiators and igniters are used in a wide variety of applications in both the civilian and military sectors. These applications include airbag triggering systems [1, 2], micropropulsion systems for microsatellites [3], and military ordnance [4, 5]. Two classes of such igniters are spark gaps and bridge wires. Spark gaps consist of two electrodes that are separated by a small distance, typically a fraction of a millimeter to a few millimeters. A high voltage, but relatively low current, is passed across these two electrodes resulting in an electrical breakdown spark-over. This ignites a relatively sensitive component of the energetic material and subsequently relies on propagation for the remainder of the material to ignite [5–7]. Bridge wires, on the other hand, consist of a thin wire that is designed to ignite energetic material from ohmic heating or wire vaporization [8, 9].

The current methods of fabrication for bridge wires and spark gaps are time-consuming and tedious; many devices are fabricated by hand. This study explores the development of printed igniters that are fabricated using a piezoelectric inkjet printer. This method has proven to be an easy and efficient means for rapid production, while allowing for a wide material selection [10–12]. A printed bridge wire or spark gap has the advantages of automated fabrication, low cost, and device-to-device performance repeatability at scale, provided certain conditions are met. Additionally, it has been demonstrated that some energetic materials, when made into a dispersion, can also be utilized in an inkjet printing system, allowing for rapid system integration [13, 14].

Other methods of printing, such as lithography, flexography, gravure, and screen printing, rely on repeatedly transferring the ink to the substrate using a previously built master pattern. Inkjet printing uses the deposition of drops to additively build up a pattern. This allows the pattern to be changed with each print, which is difficult to realize with other methods [15].

This work used a flexible polyethylene terephthalate based substrate that promotes adhesion between the substrate and ink, which allowed for a conductive trace without the need for thermal curing. Fabrication of the igniters without thermal curing was ideal to smooth the transition between silver printing and energetic material printing in the manufacturing process.

Received Feb. 28, 2018; accepted for publication May 6, 2018; published online June 11, 2018. Associate Editor: Kye-Si Kwon.
1062-3701/2018/62(4)/040406/6/$25.00

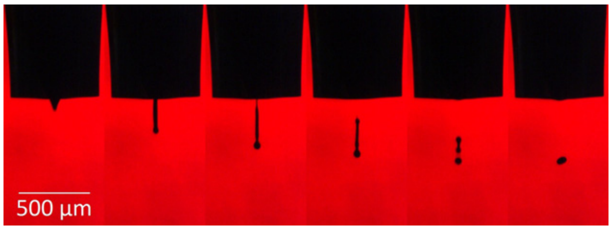

Figure 1. Drop formation of the Metalon silver nanoparticle ink at 40 V, 1100 Hz as imaged from a side mounted camera (Edmund Optics, EO-1312 Color) with telecentric lens (3x, 110 mm WD).

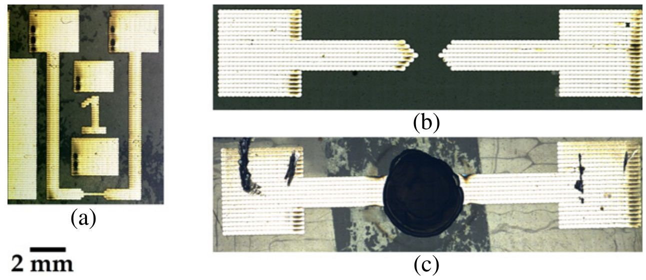

Figure 2. (a) A bridge wire and (b) a 0.85 mm spark gap both printed with a single layer of an aqueous dispersion of silver on a flexible, mesoporous medium using a MicroFab piezoelectric inkjet printer. (c) Nanothermite printed on a spark gap, covering both electrodes, with a BioFluidix piezoelectrically actuated pipette.

The objective of this work was to explore the use of piezoelectric inkjet printing as a means of rapidly fabricating printed spark gap and bridge wire igniters. The geometric features of the spark gaps were varied to determine the effect of the gap width on spark-over voltage. Similarly, the bridge wire length was varied to investigate the effect of wire length on break time. Both types of devices were then functionalized with an inkjet-printed nanothermite to validate their respective performance as an ignition mechanism for energetic material.

2. EXPERIMENTAL METHODS

2.1 *Sample Preparation*

The igniters in this work were fabricated with a piezoelectric inkjet printer (MicroFab MJ-AL-01-80) secured above a dual-axis linear positioning stage (Aerotech Planar DL 200-XY, 200 mm travel, 0.5 µm accuracy). The stage and nozzle were controlled with an in-house LabView program that coordinated the firing of the nozzle with the location of the stage. This resulted in the development of printed geometries using a raster printing path built from bitmap images in which each bit corresponded to five drops of silver ink. The samples were printed on a flexible, mesoporous printing medium (NovaCentrix, IJ-220) with aqueous dispersion of silver nanoparticles (NovaCentrix, JS-B25HV, 25 wt% Silver) filtered with a 1 µm filter (Chroma Fil Extra, GF-100/25). This substrate was used due to its polymer coating, which promotes adhesion. In addition, the wicking ability of the substrate eliminated the need for thermal curing, as it removed the solvent immediately after printing. The samples were printed with a firing voltage of 35–55 V and a firing frequency of 1–1.2 kHz. The voltage, pulse width, and firing frequency were tuned until optimal firing settings were found through side-view imaging (see Figure 1), wherein drops with compact tails and limited satellite droplets were desired. The droplet volume was approximately 90 pL. Samples were fabricated with a single layer of printed material, approximately 80–100 µm thick as observed with a 3D Optical Profiler (Zeta Instruments, 10x lens). The stage printed the samples row by row from left to right with a forward speed of 2 mm/s and a reverse speed of 8 mm/s. After printing, the samples were allowed to cure at room temperature for 24 h.

Bridge wires (Figure 2(a)) were printed with three different wire lengths, nominally 1.08 mm, 1.62 mm, and 2.16 mm. Spark gaps (Fig. 2(b)) were fabricated with three different gap widths: nominally 0.5 mm, 0.85 mm, and 1.7 mm.

Select samples were further doped with energetic material to test the effectiveness of the device as an igniter. For the spark gaps, nano-copper (II) oxide (Sigma Aldrich, 50 nm) and nano-aluminum (NovaCentrix, 80 nm, 82% active aluminum) were suspended in dimethylformamide (DMF) with polyvinylpyrrolidone to achieve an 8% solids loading. For the bridge wires, nano-bismuth (III) oxide (Nanophase Technologies Corporation, 38 nm) and nano-aluminum were suspended in DMF with Solsperse to achieve an 8% solids loading. Either mixture was then mixed with an acoustical mixer (LabRAM) for 16 min. The material was printed with a 500 µm piezoelectrically actuated pipette (BioFluidix, PipeJet P9). The material was printed using the aforementioned dual-axis linear positioning stage so that the nanothermite was deposited directly on the spark gap or bridge wire; see Fig. 2(c).

2.2 *Sample Testing*

To test the bridge wires, a custom circuit was designed and fabricated to pulse power through the device with the functional schematic shown in Figure 3. (Note that the decoupling capacitors, integrated circuit [IC] power supply connections, and a trigger conditioning circuit [two series inverting Schmitt trigger stages] have been omitted from the figure for clarity.) A function generator (Agilent 33210A) was used to produce a logic-level (3.3 V logic high, 0 V logic low) pulse with a duration of 10 ms. This voltage pulse drove a gate driver (Fairchild Semiconductor FAN3180, peak source and sink current of 2.5 A) integrated circuit, which in turn drove the base of a high-current N-channel metal–oxide–semiconductor field-effect transistor (MOSFET; International Rectifier IRFR2405). The gate driver was critical for turning on the MOSFET quickly. The output rise time of the MOSFET was measured with an oscilloscope to be less than 1 µs. The MOSFET had its source connected to the ground and a drain connected to the low side of the test device. The test device was incorporated into the circuit by sliding the printed contacts

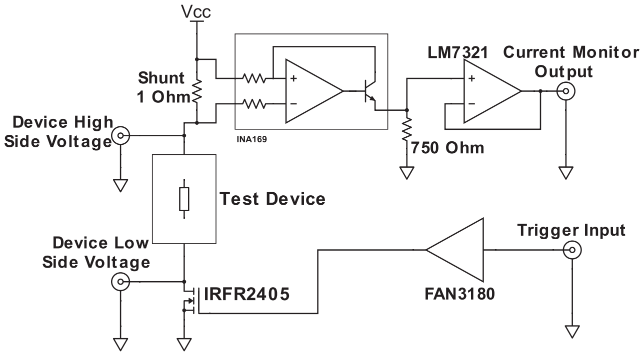

Figure 3. A schematic of the test circuit used for bridge wire characterization.

into a gap containing spring contacts for the pulse circuit. A shunt resistor array (eight 8 Ω resistors in parallel) with a total parallel resistance of 1 Ω was connected in series between the power supply and the device under test. A Texas Instruments INA169 high-side measurement current shunt monitor IC was connected across the resistor array, and a 750 Ω load resistor on the current shunt monitor output produced a measurement gain of 0.75 V/A. Estimated from the manufacturer datasheet, the current measurement bandwidth at this gain should be higher than 1 MHz. A Texas Instruments LM7321 operational amplifier served as a unity gain output buffer to the data acquisition system. The power supply could be driven from a minimum input of 5 V to a maximum input voltage of 18 V, due to the power supply being shared between all of the ICs, with the limiting device being the FAN3180 gate driver.

Four signals were measured simultaneously by an Agilent DS6014A 100 MHz bandwidth oscilloscope: (i) the function generator pulse signal, (ii) the high-side current shunt monitor output V_I, (iii) the test bridge wire high-side voltage V_H, and (iv) the test bridge wire low-side voltage V_L. These channels were all recorded using a single-shot measurement triggered on the pulse and configured to have a sub-microsecond sampling period, with the voltage ranges of the individual channels configured to maximize the dynamic range of the signal relative to the input voltage range without saturating the input. The data was saved as a time series for each initiation event, and the instantaneous differential device voltage $V_d = V_H - V_L$ was computed, as well as the instantaneous current $I_d = 0.75V_I$. The instantaneous power was computed as $P_d = V_d I_d$ and plotted as a time series. The effect of the input power on the failure of the bridge wire was determined by varying the input voltage from 7.5 V to 13.75 V in increments of 1.25 V (power source: Agilent E3634A).

The spark gaps were tested with a high-voltage power supply (Stanford Research Systems, PS365) with the maximum voltage and current set at 5.2 kV and 50 μA, respectively. The power supply was connected to the samples at the square pads using flat alligator clips. The power supply was connected to an oscilloscope to monitor the maximum voltage and current required for spark-over. To test the samples, the voltage output on the power supply was slowly ramped up until spark-over occurred, or the maximum voltage was reached. This test was repeated for samples of varying gap widths.

Table I. The effects of bridge wire length on failure.

Length (mm)	1.08	1.62	2.16
Average failure time (ms)	1.63	1.09	1.10
Failure range (ms)	(0.55, 4.7)	(0.79, 2.1)	(0.80, 1.4)
Voltage (V)	6.36 ± 0.5	6.68 ± 0.3	6.55 ± 0.2
Current (A)	1.21 ± 0.4	0.97 ± 0.2	1.09 ± 0.1
Resistance (Ω)	5.54 ± 2.8	7.04 ± 1.6	6.01 ± 0.7
Power (W)	7.62 ± 2.0	6.44 ± 1.0	7.16 ± 0.5
Samples	5	7	6

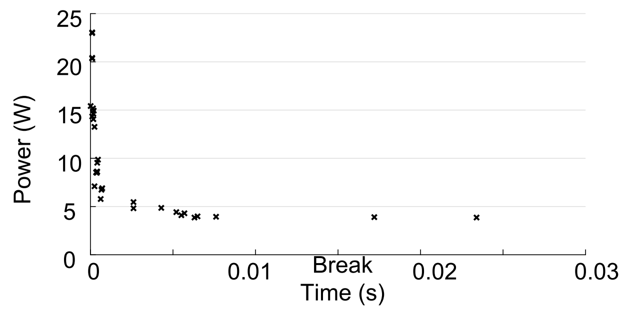

Figure 4. The average power through the 1 mm bridge wire compared to failure time.

3. RESULTS

3.1 *Electrical Characterization*

3.1.1 *Bridge Wires*

The voltage, current, and time needed to break a bridge wire for three lengths tested are shown in Table I.

The time to failure of the bridge wires with a length of 1 mm is presented in Figure 4, wherein the input power was varied and the corresponding failure time was determined.

The resistance of the whole bridge wire circuit was calculated using the obtained current and voltage data and was found to be between 4.3 and 9.1 Ω. Resistivity, ρ, was found using $\rho = RA/l$, where the resistance, R, area, A, and length, l, are as reported. The average resistivity was 26 μΩ · cm. When compared to the bulk resistivity of silver, 1.59 μΩ · cm, this method does not appear promising. However, upon comparison with other printed silver electronics, the performance of the samples described herein is acceptable. It has been reported that printed silver can have resistivities ranging from 12 to 150 μΩ · cm based on the substrate, thermal curing, and geometric consistencies of the material [16–18]. This work is on the low end of the reported range, even in the absence of thermal curing, and as such, it is claimed that the printed performance of these devices is on par with that of other printing approaches.

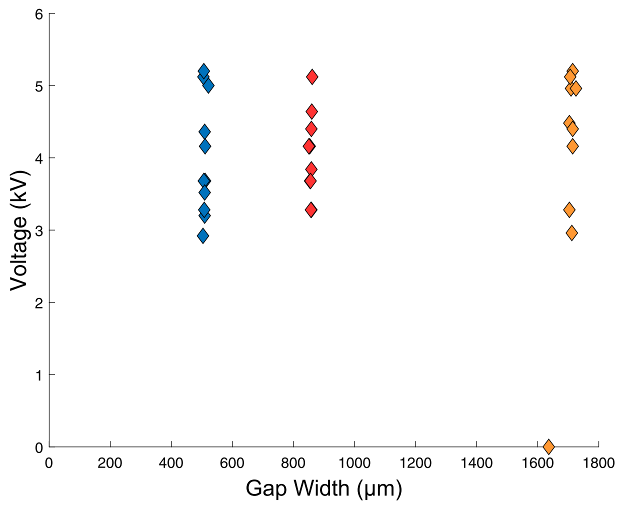

Figure 5. The voltage required for a spark discharge across the three different spark gap widths. 30 of 31 samples exhibited a spark-over behavior.

Table II. The estimated breakdown voltage for three spark gap widths in air for needle- and sphere-like electrodes. These approximations begin to break down for gap widths below 1 mm because gaseous and surface discharges begin to play a role [20].

Gap width	Needle-like electrodes	Sphere-like electrodes
0.5 mm	1.2 kV	2.42 kV
0.85 mm	1.55 kV	3.75 kV
1.7 mm	2.4 kV	6.79 kV

3.1.2 *Spark Gaps*

The voltages required for spark-over for all of the spark gaps tested, without deposited energetic material, are reported in Figure 5. 30 of the 31 samples tested successfully sparked below the 5.2 kV maximum voltage threshold. Previous modeling had been conducted for the breakdown in air with sub-millimeter electrode gaps [19] and gap widths in the millimeter to centimeter range [20]. The estimates for breakdown voltages for flat or large radius spherical electrodes and sharp, needle-like electrodes in air are given by $V = 3pd + 1.3\sqrt{d}$ and $V = pd + 0.7$, respectively, where d represents the gap width (mm), p represents the atmospheric pressure (atm), and V is the breakdown voltage (kV) [20]. The importance of the electrode geometry is due to the localization of the energy at the electrode tip. It is theorized that an electrode with a small point will require a smaller voltage to spark over due to the localization of the charge. The validity of these approximations is very sensitive to the environment in which a spark gap is tested; these effects have been investigated thoroughly [21]. The expected spark-over voltages for each gap width tested in this work when modelled as a needle-like or sphere-like electrode are included in Table II.

3.2 *Igniter Testing with Energetic Material*

To demonstrate the effectiveness of the bridge wires as igniters for energetic material, samples with a 1 mm bridge wire length were functionalized with printed nanothermite: aluminum bismuth (III) oxide. The ignition was captured with a high-speed camera (Phantom v7.0, 20,000 fps), as seen in Figure 6. The input voltage for these tests was set to 13.75 V, which is the highest voltage tested. Successful ignition of the nanothermite was observed. Due to the support system and the flexible nature of the substrate, the ignition caused the observed bending of the substrate.

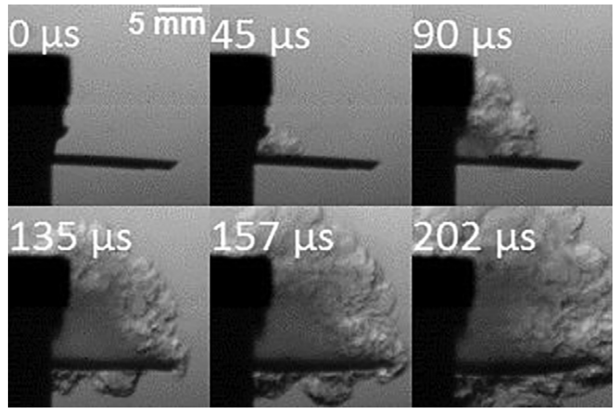

Figure 6. High-speed video schlieren images of the ignition of nano-aluminum and nano-bismuth (III) oxide obtained with a printed igniter excited at 13.75 V using the test circuit detailed in Fig. 3. The observed failure time was 70 μs.

The spark gaps were subsequently tested with deposited nanothermite, in this case, aluminum copper (II) oxide. The nanothermite ignited for 7 of 10 samples tested with the current and voltage limits at 75 μA and 5.2 kV, respectively. Figure 7 demonstrates the ignition of the deposited energetic material with the printed spark gap. In Fig. 7(b), the spark jumps over the energetic material between the two electrodes. In the second high-speed video frame (Fig. 7(c)), the printed energetic material ignites at two nodes of the spark gap. The final frame (Fig. 7(d)) shows a single flame from the union of the two initial ignition points.

4. DISCUSSION

The manufacturing technique described in this work has provided a solution for fabricating metallic initiators on flexible substrates. They can be directly functionalized with energetic material due to the lack of thermal curing required in the fabrication process. This offers inherent benefits when compared to the traditional inkjet printing of metals, which requires high-temperature sintering. As such, both the spark gaps and bridge wires fabricated in this manner can be part of a fully printed solution with deposited energetic material to rapidly fabricate precise igniters.

For the spark gaps, it was found that the width of the gap is a critical design factor due to its correlation with spark-over voltage. In addition, the shape of the electrode printed is critical for accurately predicting the spark-over voltage; the voltage needed decreases with the sharpness of the electrode point. Arguably, the variability of the voltage data for a single gap width in this work can be attributed, in part, to the slight variations in the printed electrode shape.

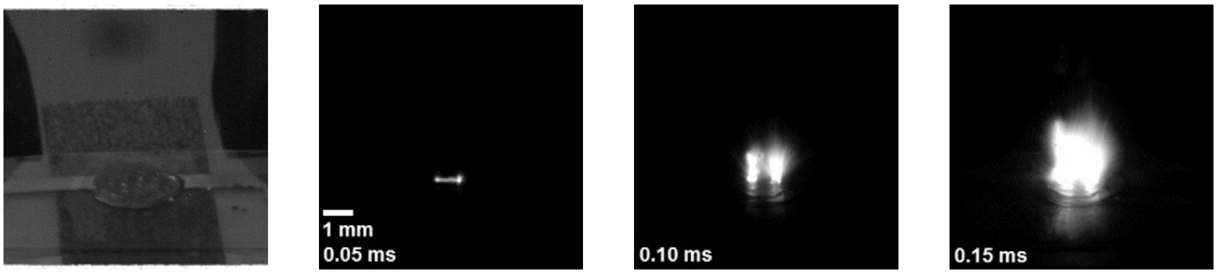

(a) (b) (c) (d)

Figure 7. (a) Unreacted nanothermite printed on a spark gap. (b)–(d) High-speed video images of the ignition of the printed nanothermite with a printed spark gap.

On the other hand, the key criterion for the bridge wires was the consistency of the deposited material to produce low-resistance devices. The resistance of the device was highly correlated to the precision of the geometric features and sufficient solvent evaporation. Due to the nature of the inkjet process, there was wide variability in the resistance of the various bridge wires, and thus the power required for failure. The manufacturing defects can be worked around if the voltage delivered by the power source in these devices is higher than the expected threshold of the lower quality bridge wires produced. Further work fine-tuning the fabrication process and defining a narrower input power range is critical before the bridge wires can be reliably implemented.

The spark gaps developed were effective mechanisms for the ignition of energetic material. The limitation to these mechanisms, however, was the miniaturization of the high-voltage power source and the environment's influence on the breakdown voltage. Overcoming these obstacles with efficient packaging could prove non-trivial. However, in applications where space or power is not a limiting factor, these devices would be advantageous.

When compared to each other, spark gaps and bridge wires offer complementary but unique benefits. Both devices can be fabricated relatively quickly with high precision through the use of inkjet printing. As such, they can be functionalized directly with energetic material in the fabrication process. Bridge wires require low voltages, and as such, the entire igniter system can be easily miniaturized. However, the spark gaps' large voltage requirement could make packaging the device non-trivial. The uniqueness of these igniters ultimately lies in the energetic material that they can be implemented with. Bridge wires work better with an energetic material that is shock or heat sensitive, while spark gaps are more effective with energetic materials that are sensitive to electrostatic discharge.

Both spark gaps and bridge wires were successful in igniting energetic material. They can be developed into fully printed igniters; however, there is more work to be done with regard to their reliability. In addition, it is imperative that the sensitivity to accidental ignition be studied with these devices before their true feasibility can be assessed.

5. CONCLUSIONS

In this work, spark gaps and bridge wires were fabricated with inkjet printing as means to develop ignition systems for energetic material. The spark gaps offer an effective ignition mechanism for energetic material that is sensitive to electrostatic discharge. It is acknowledged that fine-tuning the performance of the system would be essential for implementation and enhancing the reliability. On the other hand, the bridge wires tested here proved to be most sensitive to the power input. A correlation between input power and failure time for the bridge wires was developed. The devices in this study have proven effective for the ignition of nanothermite. The work herein is intended as a demonstration of the fabrication process and a comparison of the ignition mechanisms. The repeatability of a single device was not investigated because both the spark gaps and bridge wires were designed to be single-use igniters. However, future studies on reliability and manufacturing controls are required.

ACKNOWLEDGMENTS

The authors would like to thank Christopher J. Morris for his helpful and constructive input. This research is supported by the U.S. Department of Defense, Defense Threat Reduction Agency through grant number HDTRA1-15-1-0010 and is managed by Dr. Allen Dalton. The content of the information does not necessarily reflect the position or the policy of the U.S. federal government, and no official endorsement should be inferred.

REFERENCES

1 A. Hofmann, H. Laucht, D. Kovalev, V. Timoshenko, J. Diener, N. Künzner, and E. Gross, "Explosive composition and its use," US Patent 6,984,274 (2006).
2 J. H. Evans, "Airbag igniter and method of manufacture," US Patent 5,639,986 A (1997).
3 D. H. Lewis, S. W. Janson, R. B. Cohen, and E. K. Antonsson, "Digital micropropulsion," Sensors Actuators A **80**, 143 (2000).
4 T. A. Baginski, T. S. Parker, and D. M. Fahey, "Electro-explosive device with laminate bridge," US Patent 6,772,692 (2004).
5 B. Neyer, D. R. Knick, P. T. Moore, and R. Tomasoski, "Initiator," US Patent 9,534,875 (2017).
6 J. C. Fisher, "Ignitor with printed electrostatic discharge spark gap," US Patent 6,467,414 (2002).
7 R. K. Reynolds, C. J. Nance, and A. F. Cunningham, "Plastic encapsulated energetic material initiation device," US Patent 7,690,303 (2010).

[8] R. Varesh, "Electric detonators: EBW and EFI," Propellants Explos. **21**, 150 (1996).
[9] C. S. Staley, C. J. Morris, R. Thiruvengadathan, S. J. Apperson, K. Gangopadhyay, and S. Gangopadhyay, "Silicon-based bridge wire micro-chip initiators for bismuth oxide - aluminum nanothermite," J. Micromech. Microeng. **21**, 115015 (2011).
[10] J. E. Bengston and G. B. Larson, "Method for fabricating printed circuits," US Patent 5,235,139 (1993).
[11] C. F. Coombs Jr, *Printed Circuits Handbook* (McGraw-Hill, Inc., New York, NY, 1987).
[12] H. Sirringhaus, T. Kawase, R. H. Friend, T. Shimoda, M. Inbasekaran, W. Wu, and E. P. Woo, "High-resolution inkjet printing of all-polymer transistor circuits," Science **290**, 2123 (2000).
[13] A. S. Tappan, J. P. Ball, and J. W. Colovos, Inkjet printing of energetic materials, OSTI 1118431, Sandia National Laboratories (SNL-NM), Albuquerque, NM (United States), (2011).
[14] A. K. Murray, W. A. Novotny, T. J. Fleck, I. E. Gunduz, S. F. Son, G. T.-C. Chiu, and J. F. Rhoads, "Selectively-deposited energetic materials: A feasibility study on the piezoelectric inkjet printing of nanothermites," Additive Manufacturing **22** (2018).
[15] S. D. Hoath (ed.), *Fundamentals of Inkjet Printing* (Wiley-VCH Verlag and Co., Weinheim, Germany, 2011).
[16] J. Perelaer, C. E. Hendriks, A. W. M. de Laat, and U. S. Schubert, "One-step inkjet printing of conductive silver tracks on polymer substrates," Nanotechnology **20**, 165303 (2009).
[17] A. Bonea, A. Brodeala, M. Vladescu, and P. Svasta, "Electrical Conductivity of Inkjet Printed Silver Tracks, Electronics Technology (ISSE)," *35th Int'l. Spring Seminar* (IEEE, Piscataway, NJ, 2012), pp. 1–4.
[18] A. Arazna, K. Janeczek, and K. Futera, "Mechanical and thermal reliability of conductive circuits inkjet printed on flexible substrates," Circuit World **43**, 9 (2017).
[19] C.-H. Chen, J. A. Yeh, and P.-J. Wang, "Electrical breakdown phenomena for devices with micron separations," J. Micromech. Microeng. **16**, 1366 (2006).
[20] M. Mardiguian, *Appendix C: Spark-Over Voltages, Electrostatic Discharge* (John Wiley & Sons, Inc., New York, NY, 2016).
[21] S. Bönisch, D. Pommerenke, and W. Kalkner, "Broadband measurement of ESD risetimes to distinguish between different discharge mechanisms," J. Electrost. **56**, 363 (2002).